Surface Science 749 (2024) 122550

Contents lists available at ScienceDirect

Surface Science

journal homepage: www.elsevier.com/locate/susc

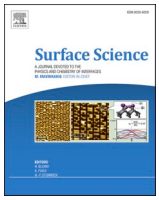

Infrared Reflection-Absorption Spectroscopy (IRRAS) applied to oxides: Ceria as a case study

Chengwu Yang [a], Christof Wöll [b,*]

[a] School of Energy and Power Engineering, Beihang University, Beijing 100191, China
[b] Institute of Functional Interfaces, Karlsruhe Institute of Technology (KIT), Karlsruhe 76021, Germany

ARTICLE INFO

Keywords:
IRRAS
Ceria
Single crystal

ABSTRACT

Infrared Reflection-Absorption Spectroscopy (IRRAS), a pivotal tool in the study of the surface chemistry of metals, has recently also gained substantial impact for oxide surfaces, despite the inherent challenges originating from their dielectric properties. This review focuses on the application of IRRAS to ceria (CeO_2), a metal oxide for which a significant amount of experimental data exists. We elaborate on the differences in optical properties between metals and metal oxides, which result in lower intensity of adsorbate vibrational bands by approximately two orders of magnitude and polarization-dependent shifts of vibrational frequencies. We examine how the surface selection rule, governing IR spectroscopy of adsorbates on metals, contrasts sharply with the behavior of dielectrics where both positive and negative vibrational bands can occur, and how IRRAS can capture vibrations with transition dipole moments oriented parallel to the surface—a capability not feasible on metallic surfaces. Finally, this paper explores the broader implications of these findings for enhancing our understanding of molecule interactions on oxide surfaces, and for using IR spectroscopy for operando studies under technologically relevant conditions.

1. Introduction

The application of Infrared Reflection-Absorption Spectroscopy (IRRAS) has proven highly successful in elucidating the chemical and physico-chemical properties of metal surfaces by investigating the vibrational characteristics of adsorbates [1]. While virtually all metals across the periodic table have been examined using this crucial variant of vibrational spectroscopy, much less information is available for metal oxides. This scarcity is not due to a lack of interest; in fact, there is a bulk of work on oxide powders where reference data for single crystals is urgently needed [2]. Instead, this lack of information stems from experimental challenges arising from the distinct properties of dielectric surfaces concerning the reflection and refraction of light. The optical properties of dielectrics show substantial differences from metals, resulting in a significant reduction in the intensity of adsorbate vibrational bands observed in IRRAS—approximately by two orders of magnitude [3]. For this reason, the first experimental IR spectra recorded in reflection for a metal oxide surface were reported as late as 1999 [4], with substantial progress emerging only in the past decade. As a result of the rather incomplete characterization of adsorbate vibrations an understanding of oxide surface chemistry is lacking behind that achieved for metals, where the so-called Surface Science approach was extremely successful [5].

This review demonstrates the particular properties of IRRAS studies on metal oxide single crystal surfaces by using ceria (CeO_2) as an example, because for this material the largest amount of IRRAS data recorded for bulk single crystals, or monocrystals, is currently available. We will use this important rare earth metal oxide to discuss the often-counterintuitive results obtained for the sign, the position, and the shape of IR bands related to vibrations of adsorbates on oxide surfaces.

The reflection of light from metal surfaces is governed by the screening of the electric field by the metal electrons. For the s-polarized component (E_s in Scheme 1) and the p-polarized component ($E_{p,t}$ in Scheme 1), both oriented parallel to the surface plane, this interaction results in the formation of an image dipole, which effectively cancels out all components of the electric field parallel to the surface. Consequently, adsorbate vibrations with a transition dipole moment oriented parallel to the surface are not detectable on metal surfaces or surfaces exhibiting metallicity.

For the component $E_{p,v}$ polarized normal to the metal surface (see Scheme 1) the situation is completely different. For metals, in this case the image dipole is oriented in the same direction as the incident $E_{p,v}$

* Corresponding author.
E-mail address: christof.woell@kit.edu (C. Wöll).

https://doi.org/10.1016/j.susc.2024.122550
Received 10 June 2024; Received in revised form 8 July 2024; Accepted 10 July 2024
Available online 14 July 2024

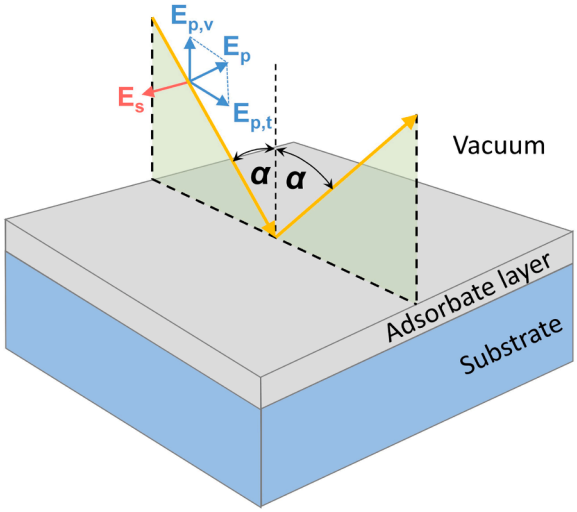

Scheme 1. Schematic view of the decomposition of the incident E-vector into three different components. Note that for s-polarized light, E_s, only one component has to be considered, for p-polarized light the vector E_p has to be decomposed in the $E_{p,v}$ and $E_{p,t}$.

component, i.e. normal to the surface, thus enhancing the total electric field rather than compensating it. As a result, the intensity of vibrational bands with transition dipole moments oriented perpendicular to the surface is strongly enhanced. Together with the screening of the component parallel to the surface these boundary conditions lead to the so called "surface-selection" rule that states that for adsorbates on metal surfaces or surfaces which show metallicity only vibrations with a substantial component of their transition dipole moment oriented perpendicular to the surface can be seen [6]. This surface selection rule has been often applied in Surface Science to infer on the orientation of molecules on metal substrates [1]. On the other hand, it is also a restriction since adsorbate vibrations with their TDM oriented parallel to the surface are invisible. In addition, there is no dependence on azimuthal incidence angle, rotating the sample around its surface normal will not change the spectra. Any azimuthal alignment occurring e.g. on substrates with two-fold symmetry can thus not be detected.

On metal oxides and dielectrics in general, the situation is quite different. These materials are insulators, and as a result, in the infrared and visible regimes, screening by metal electrons cannot occur. Therefore, the optical properties of metal oxide substrates deviate substantially from those of metals. The most experimentally relevant consequence is that intensities of adsorbate vibrational bands are strongly reduced, typically by two orders of magnitude.

In 1963, Becket and Gobeli [7] were the first to demonstrate that the limitations restricting the application of IRRAS to adsorbates on dielectric substrates could be addressed by using multiple internal reflections (MIR). In specially shaped samples as many as 20 reflections can be utilized to amplify the absorption of adsorbate vibration bands. Specifically, for Si, where the production of single crystals with the necessary geometries is feasible and where the overall absorption of IR radiation in the bulk is sufficiently low, they were able to detect the faint Si−H stretching mode observed using MIR. For a review of MIR, see [8].

It should also be noted that, in addition to enhancing the sensitivity of IR spectroscopy to adsorbate vibrations through multiple reflections, the internal reflection geometry allows the analysis of all components of surface vibrations with comparable sensitivity, including vibrations with their transition dipole moment (TDM) oriented both parallel and perpendicular to the surface. However, very few materials are suitable for producing the required special shaped samples, with Si and Ge being the primary examples. This approach using internal reflections is infeasible for metal oxides, as their transmission in the IR regime is not sufficiently high.

As a result, only externally reflected IR light can be used to study adsorbates on metal oxide surfaces. However, due to technical difficulties, it was not until 1999 that the first surface adsorbate vibration on a metal oxide was detected using IRRAS on a rutile TiO_2(110) substrate [4].

The relatively low intensities of vibrational bands in IRRAS data for oxides compared to metals is just one distinction – dielectrics also exhibit several other, occasionally unexpected and surprising, characteristics when external reflection of IR light to detect molecular vibrations.

First, the sign of the vibrational bands is not always negative as in the case of metals, where the interaction of IR-light with a molecular vibration always leads to an absorption band, i.e. a reduction of reflected intensity. On dielectrics, vibrational bands can be either positive or negative depending on conditions [9]. The somewhat counterintuitive increase of reflectivity occurring when exciting a molecular vibration is due to the complex interference phenomena occurring at surfaces of dielectrics [8]. Although this behavior is reproduced by semiempirical [10] as well as by full ab-initio calculations [11], a simple explanation is presently lacking. Note, that in transmission bands are always positive (i.e. transmission intensities decrease when exciting a molecular vibration). Second, spectra can also be recorded using s-polarized light, which makes it possible to observe vibrations with their transition dipole moments oriented parallel to the surface. The same is true for the component of the p-polarized light oriented parallel to the surface, $E_{p,t}$ in Scheme 1. Third, a splitting of bands can be observed in p-polarized light. This was experimentally first demonstrated for H/Si(100) [12], and later for CO on MgO and CeO_2(111) [13]. While the size of the shift amounts to only ~4 cm^{-1} for CO and of ~1 cm^{-1} for SiH, for large transition dipole moments (TDM) shifts of up to 30 cm^{-1} have been seen for CO_2 [11] and N_2O [10]. As noted above for the sign reversal of vibrational bands, this shift is reproduced by semiempirical [13] and ab-initio calculations [11], but a simple explanation has not yet been presented. This shift of frequencies fact has to be considered when comparing experimental data to predictions of vibrational frequencies obtained from electronic structure calculations (e.g. density functional theory, or DFT). The frequency of the bands observed with $E_{p,v}$ light are always "dressed", a comparison to results of frequencies based on electronic structure calculations requires the non-shifted frequencies measured either in s-polarization or with the $E_{p,t}$ component. Only when using a full ab-inito approach using a thorough description of the electromagnetic coupling at dielectrics, a direct comparison between experimental data and theoretical results becomes possible [11].

In addition, for the vibrations coupling to E_s and $E_{p,t}$ the IRRAS data will show a dependence on the azimuthal angle for dielectric materials. For substrates with two-fold symmetry, this fact allows for the detection of adsorbate azimuthal alignment [14].

In this review, we will examine the case of CeO_2 to discuss the key differences between metals and oxides in IR spectra recorded in reflection, which are crucial for interpreting IRRAS data to the study of molecule interactions with oxide monocrystal substrates.

1.1. Ceria

Ceria, or cerium dioxide (CeO_2), is a versatile and intriguing material well beyond its well-known applications in heterogeneous catalysis. This rare earth oxide is distinguished by its unique electronic properties, such as filled 4f states localized at the Ce^{3+} ions, [15,16] and a fluorite crystal structure, which contributes to its wide range of applications in various fields. Understanding the structural nuances and the resulting chemical properties of these surfaces is crucial, as they profoundly influence ceria's properties and interactions in various applications, including but not limited to catalysis, such as in solid oxide fuel cells, polishing powders, oxygen sensors, UV absorbers, and in the biomedical field. The rich interplay between ceria's crystal structure and surface

characteristics opens up a broad spectrum of possibilities for its use in advanced technological applications.

Ceria crystallizes in a cubic fluorite structure, characterized by a simple and highly symmetric arrangement. This structure is pivotal in defining its chemical and physical properties. The fluorite structure of ceria consists of cerium ions (Ce^{4+}) occupying a face-centered cubic lattice and oxygen ions (O^{2-}) filling the tetrahedral interstices.

In ceria, the low Miller-indexed surfaces, specifically the (111), (100), and (110) surfaces, showcase varied stability and electronic properties [17]. The nonpolar (111) surface emerges as the most stable among them. This surface is characterized by a close-packed arrangement, forming a three-layer repeating sequence, which effectively minimizes surface energy, thereby enhancing its stability. On the other hand, the (100) surface presents a more open structure and possesses a higher surface energy compared to the (111) surface. Its inherent polarity can lead to potential instabilities and a tendency for surface reconstructions under different conditions. Meanwhile, the nonpolar (110) surface, marked by rows of oxygen and cerium atoms, strikes a balance in terms of polarity and stability. It stands in a middle ground, being less stable than the (111) surface but demonstrating more stability than the polar (100) surface.

2. Ceria's role in heterogeneous catalysis

Ceria (CeO_2) is a versatile material in the realm of heterogeneous catalysis, owing to its remarkable redox characteristics, ability to store and release oxygen, and its unique acid-base properties [18–20]. Ceria is commonly used as an active component or support in catalysts to facilitate a wide range of redox and acid-base catalytic reactions. These properties make ceria a critical component in applications like vehicle emission control, chemical transformations, and even photocatalysis.

3. Creation of oxygen vacancies on ceria surfaces

A primary factor contributing to the significance of ceria in heterogeneous catalysis is its relatively low energy requirement for creating oxygen vacancies, compared to those of all other commonly used transition and rare earth metal oxides [21]. The energy required to create oxygen vacancies in ceria varies significantly across its different crystallographic orientations - (111), (100), and (110) [21,22]. Each of these orientations has unique surface properties that influence their ability to form oxygen vacancies, a key factor in their catalytic activity.

On the CeO_2 (111) surface, known for being the most stable, the energy required to form oxygen vacancies is relatively low. This is due to its close-packed structure, which naturally minimizes surface energy, making the formation of vacancies more energetically favorable [21, 22]. This characteristic makes the (111) surface highly efficient in redox reactions, a core aspect of heterogeneous catalysis.

Conversely, the CeO_2(100) surface, distinguished by its open and polar characteristics, displays a higher surface energy. As a result, creating oxygen vacancies on this surface requires less energy than on the (111) surface. This reduced energy demand can influence the surface reactivity and the pace of catalytic reactions. Meanwhile, the CeO_2(110) surface balances between the (111) and (100) surfaces in stability, requiring the least energy for forming vacancies [21,22].

The role of oxygen vacancies in ceria, particularly their location in the crystal lattice, is currently a subject of ongoing debate among researchers. This discussion primarily revolves around the thermodynamic stability of these vacancies, whether they are most stable when situated in the top layer or embedded deeper in the second layer of the crystal structure. This aspect of oxygen vacancy placement varies across the different crystallographic surfaces of ceria, namely the (111), (110), and (100) surfaces, each exhibiting unique characteristics [23].

For the CeO_2 (111) surface, some studies suggest that oxygen vacancies may preferentially form in subsurface regions. In contrast, for the CeO_2 (110) and (100) surfaces, experimental works have provided evidence that here the oxygen vacancies are indeed located in the top layer.

Ceria entered the realm of heterogeneous catalysis in 1976 when Ford Motor Company first incorporated it into three-way catalysts for controlling vehicle emissions [24]. This application remains ceria's most notable success in catalysis, consuming about 20 % of its annual production. Since its introduction, ceria has demonstrated strong performance in various chemical reactions, including redox, acid-base, and photocatalytic reactions, with particular prominence in catalyzing redox reactions. The effectiveness of ceria-based catalysts in redox reactions stems from their capacity to release and absorb oxygen within their lattice structure. A deep understanding of the dynamics of O vacancy formation is crucial for developing and optimizing catalysts that are vital for energy production and environmental protection.

In this context it is of interest to note that the presence of Ce^{3+} ions in ceria offers a unique spectroscopic signature that can be effectively monitored using infrared (IR) spectroscopy. Notably, an electronic Ce^{3+} spin-orbit transition associated with Ce^{3+} ions manifests as a distinct band at around 2135 cm^{-1} in the IR spectra [25]. This feature provides a valuable opportunity for real-time observation and analysis of oxygen vacancy formation in ceria. Therefore, the ability to monitor this band allows for a direct and insightful understanding of the dynamic processes involving oxygen vacancy formation in ceria. This capability is particularly advantageous in the study of catalytic reactions and material properties, where the creation and behavior of oxygen vacancies play a critical role in influencing the performance and efficiency of ceria-based catalysts and materials.

4. IRRAS studies of adsorbates on differently oriented ceria surfaces

IRRAS studies reported during the last decade have been instrumental in gaining a deeper understanding of the surface chemistry of ceria. This technique allows for the precise determination of vibrational frequencies of various adsorbates, shedding light on the interaction dynamics at the molecular level on different crystallographic surfaces of ceria.

In addition, studies on single crystal surfaces also provide the data base for the interpretation of data recorded for powder materials, either at low pressures using transmission geometries or at high pressures up to 1 atm using the DRIFTS technique [26].

Prior to 2012, research on adsorbates on macroscopic ceria surfaces exclusively focused on ceria thin films grown on metallic substrates [17, 27]. This trend is reflective of the experimental challenges in recording IR data from bulk dielectrics and oxides. The presence of an underlying metal substrate significantly enhances the vibrational signatures in the IR data, providing an amplification factor of at least four. This enhancement results from the metal acting as a mirror, thus boosting the detectability of the adsorbate vibrational bands. However, the IR data recorded for thin oxide or ceria layers on metals is incomplete, information for vibrations oriented parallel to the substrate (i.e. vibrations excited by E_s and $E_{p,t}$) is missing.

While the presence of metal substrates supporting the ceria thin layers offers experimental advantages, it is imperative to recognize the limitations these studies present, especially in the context of validating theoretical models for the vibrational frequencies. Depending on the size of the transition dipole moments, TDM, vibrational peaks coupled to the $E_{p,v}$ component of the electric field shows a pronounced shift with respect to the "ideal" or "undressed" frequency which can only be observed for E-vector components oriented parallel to the surface, E_s and $E_{p,t}$ (see discussion above).

In case of CO_2 adsorbed on CeO_2(111), for example, these shifts are on the order of 25 cm^{-1} [11]. This fact which has to be considered when comparing experimental frequencies to computational results obtained e.g. with density functional theory (DFT). Only the band position observed in s-polarized light (or for the $E_{p,t}$ component) can be used to

validate theoretical (e.g. DFT) results. The $E_{p,v}$ component, the only contribution present for adsorbates on metals and on oxide thin films supported on metals is shifted by an amount which depends on the transition dipole moment. For CO, this shift is on the order of 4 cm^{-1}, for CO_2 and N_2O values of 20 and 25 cm^{-1} have been observed experimentally. Theoretical predictions of the "dressed" frequencies observed for vibrations coupling to the E-field component oriented vertical to the surface require accurate ab-initio calculations explicitly considering the propagation of light on the surfaces of dielectrics [11], which represents a formidable effort.

It also has to be considered that ceria thin films on metal substrates may introduce additional complexities and interactions with adsorbates that are not characteristic of macroscopic bulk ceria samples, including higher defect densities and charge transfer from the metallic substrate to the adsorbate [28,29].

Therefore, to achieve a more accurate and thorough understanding, and to robustly validate theoretical predictions for adsorbate vibrational frequencies, it is essential to conduct measurements on true macroscopic single crystals, or monocrystals, of ceria. Such an approach is crucial to provide consistent insight into the surface dynamics and interactions of adsorbates on ceria (Table 1).

4.1. $CeO_2(111)$

The vibrational dynamics at the molecular level of adsorbates on different crystallographic surfaces of ceria present valuable insights into the nature of the adsorbate dynamics and the nature (e.g. presence of oxygen vacancies and other defects) of the supporting oxidic substrate. On the CeO_2 (111) surface (see Fig. 1), the adsorbates studied with IRRAS so far include CO, which shows vibrational frequencies of 2154 cm^{-1} on fully oxidized surfaces, and 2163 cm^{-1} at Ce^{4+} ions at the vacancy site [30]. For adsorbed methanol and deuterated methanol, multiple vibrational modes were detected, such as C−O stretching (1085, 1060, 1040, 1020 cm^{-1} in Fig. 2), CD_3 s-deformation (1117 cm^{-1}), CH_3 stretching (2910, 2795 cm^{-1}), and CD_3 stretching (2068, 2038 cm^{-1}) [33]. For the fully oxidized samples, exposure to O_2 did not lead to any molecular vibration (Fig. 3). In the case of the reduced $CeO_{2-x}(111)$ substrates, the formation of activated dioxygen species (superoxo ($O_2^{\bullet-}$) and peroxo (O_2^{2-}) species) are not observed when exposed to O_2. This leads to the conclusion that on the most energetically stable (111) surface, the oxygen vacancies are actually not located in the top-plane, but must be deeper into the bulk, in full agreement with the results of previous theoretical predictions. These findings resolve a long-standing, intense debate concerning the location of the O-vacancies for the reduced $CeO_{2-x}(111)$ [34]. Fig. 4 shows the polarization-resolved IRRA spectra of 1 monolayer (ML) N_2O adsorption on the fully oxidized $CeO_2(111)$ surface at 110 K. The p-polarized spectrum shows a positive band at 2232 cm^{-1} and a negative band at 2255 cm^{-1}, while in the s-polarized spectrum only a negative band at 2234 cm^{-1} is observed. Fig. 4 also shows the polarization-resolved IRRA spectra of 1 ML N_2O adsorption on the reduced $CeO_{2-x}(111)$ surface at 110 K. The positive and negative bands in the p-polarized spectrum shift to 2231 and 2248 cm^{-1}, respectively. In the s-polarized spectrum, only a negative band is seen at 2234 cm^{-1}. These bands all originate from the asymmetric stretching vibration (ν_{as}) of the adsorbed N_2O molecules and are blue-shifted compared to the gas phase value (2224 cm^{-1}) [10].

Table 1
IRRAS measured frequency values of various adsorbates on ceria single crystal surfaces with different orientations.

Adsorbate	CeO_2 surface orientation	Frequency (cm^{-1})	Refs.	Type of vib. mode
CO	oxidized $CeO_2(111)$	2154	ref. [30]	CO stretch
	reduced $CeO_{2-x}(111)$	2163		
	oxidized $CeO_2(110)$	2170	ref. [31]	
	reduced $CeO_{2-x}(110)$	2175		
	oxidized $CeO_2(100)$	2176/2168/2147	ref. [32]	
	reduced $CeO_{2-x}(100)$	2168/2147		
CH_3OH	oxidized $CeO_2(111)$	1085/1060	ref. [33]	C − O stretch
	oxidized $CeO_2(110)$	1108		
CD_3OD	oxidized $CeO_2(111)$	1117	ref. [33]	CD_3 s-deform.
		1040/1020	ref. [33]	C − O stretch
	oxidized $CeO_2(110)$	1125	ref. [33]	CD_3 s-deform.
		1060	ref. [33]	C − O stretch
O_2	reduced $CeO_{2-x}(110)$	1130	ref. [34]	superoxo species
		885		peroxo species
	reduced $CeO_{2-x}(100)$	1129		superoxo species
N_2O	oxidized $CeO_2(111)$	2255/2232	ref. [10]	Asymmetric stretch
	reduced $CeO_{2-x}(111)$	2248/2231		
	oxidized $CeO_2(110)$	2248/2235	ref. [35]	
	reduced $CeO_{2-x}(110)$	2250/2235		
CO_2	oxidized $CeO_2(111)$	2360/2237	ref. [11]	CO_2 asym. stretch

4.2. $CeO_2(110)$

On the CeO_2 (110) surface (see Fig. 1), CO shows a vibrational frequency at 2170 $cm^{-1}$and of 2175 cm^{-1} in the vicinity of oxygen vacancy [31]. Fig. 2a shows the IRRA spectra of methanol on a fully oxidized $CeO_2(110)$ surface at 125 K. Only one intense band was observed at 1108 cm^{-1}. This band can be assigned in a straightforward fashion to the C−O stretching mode of methoxy monomers bound to the surface as monodentates. Fig. 2b shows the corresponding IRRA spectra recorded after adsorption of CD_3OD. The C−O stretching mode shifts to 1060 cm^{-1} due to the mass change from CH_3 to CD_3. The band at 1125 cm^{-1} is assigned to the CD_3 s-deformation mode [33]. Additionally, the adsorption of dioxygen on reduced ceria surfaces is characterized by vibrational bands of superoxo (1130 cm^{-1}) and peroxo (885 cm^{-1}) species (see Fig. 3), offering insights into oxygen activation mechanisms [34]. This surface demonstrates a high sensitivity to structural changes, impacting the adsorption and activation of molecular species, which is critical for catalyzing reactions. Fig. 4a shows p-polarized IRRAS data recorded after N_2O adsorption at 120 K on ceria (110) surfaces. For the fully oxidized (110) surface, the spectrum shows a dominant positive absorption band at 2235 cm^{-1} arising from the asymmetric stretching mode of N_2O. For the highly reduced $CeO_{2-x}(110)$ surface, a second, negative band at 2250 cm^{-1} becomes dominant. In this case, the ceria (110) surface exhibits a (2×1) reconstruction, with 25 % oxygen atoms missing. The new band at 2250 cm^{-1} is assigned to N_2O species adsorbed at surface O vacancies. In the s-polarized spectrum, only a much smaller negative band at 2240 cm^{-1} is observed [35].

4.3. $CeO_2(100)$

Lastly, as shown in Fig. 1, CO adsorbed on the oxidized (100) surface shows an intense band at 2176 cm^{-1} with a shoulder at 2168 cm^{-1} and a second weaker peak at 2147 cm^{-1}. Upon further reduction of the surface, a shift of the main band from 2176 to 2168 cm^{-1} is observed, while the frequency of the low-lying band remains unchanged at 2147 cm^{-1} [32]. In contrast to (111) and (110), only the vibrational band of superoxo (1129 cm^{-1}) can be detected after O_2 adsorption on the reduced ceria (100) surface (Fig. 3) [34]. The (100) surface of ceria is a polar surface. Under UHV conditions and the associated treatments, a two-step scenario occurs on the surface where an initial O-terminated (2×2) reconstruction is followed by a severe refaceting via massive mass

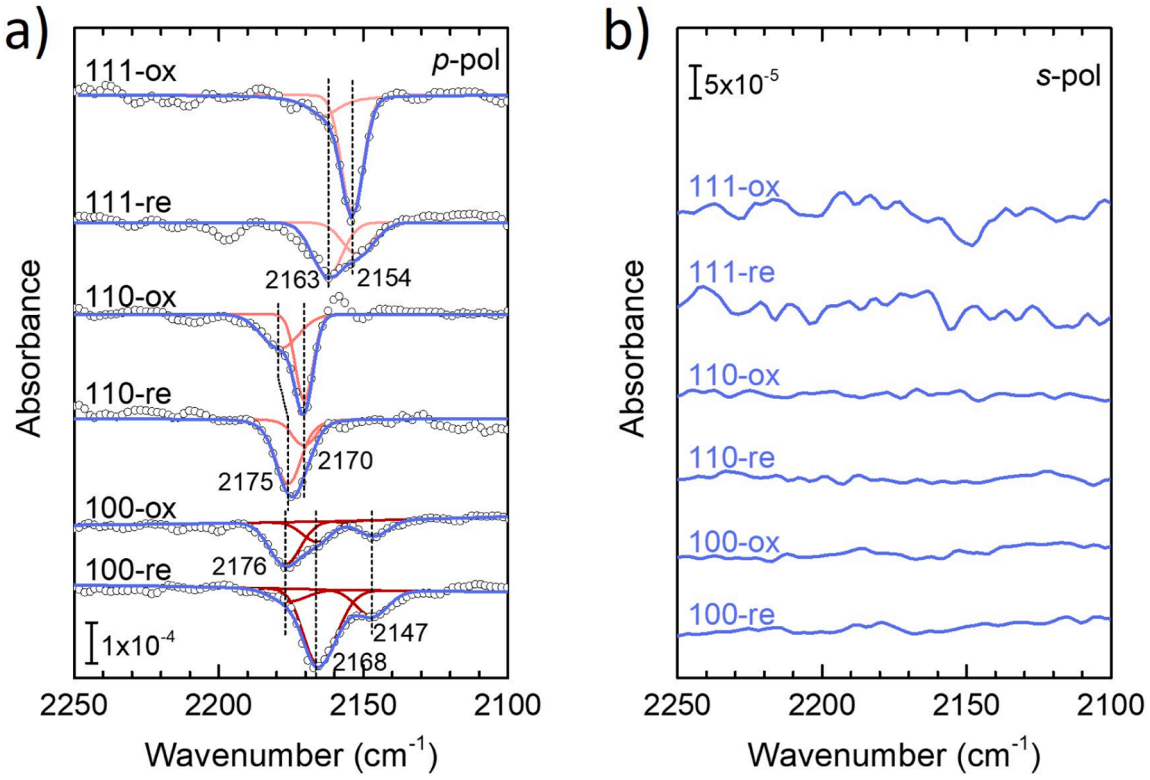

Fig. 1. Polarization-resolved IRRAS data of 1 monolayer (ML) CO adsorption on the oxidized and reduced (111), (110), and (100) ceria surfaces at about 70 K: (a) p-polarized spectra; (b) s-polarized spectra. Reproduced from Ref. [36].

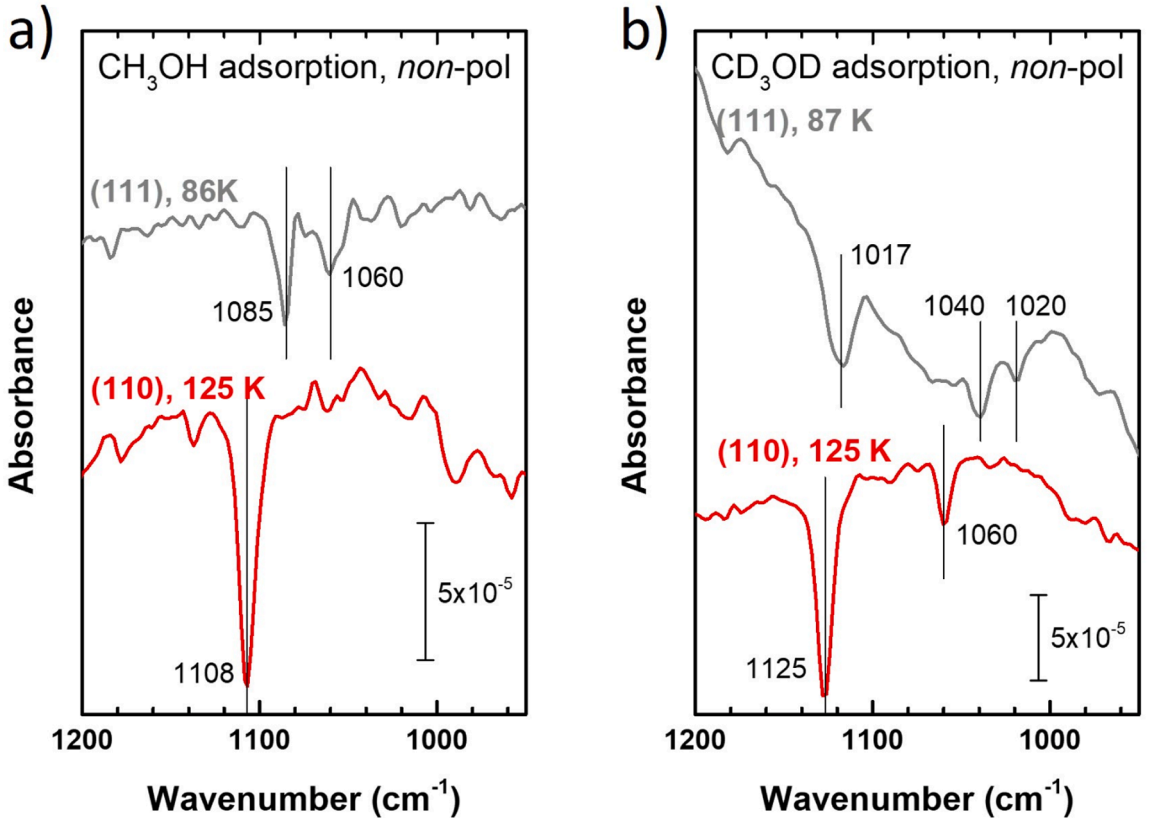

Fig. 2. IRRAS data of 1 ML CH_3OH and CD_3OD adsorption on the oxidized (111) and (110) ceria surfaces. Reproduced from Ref. [33].

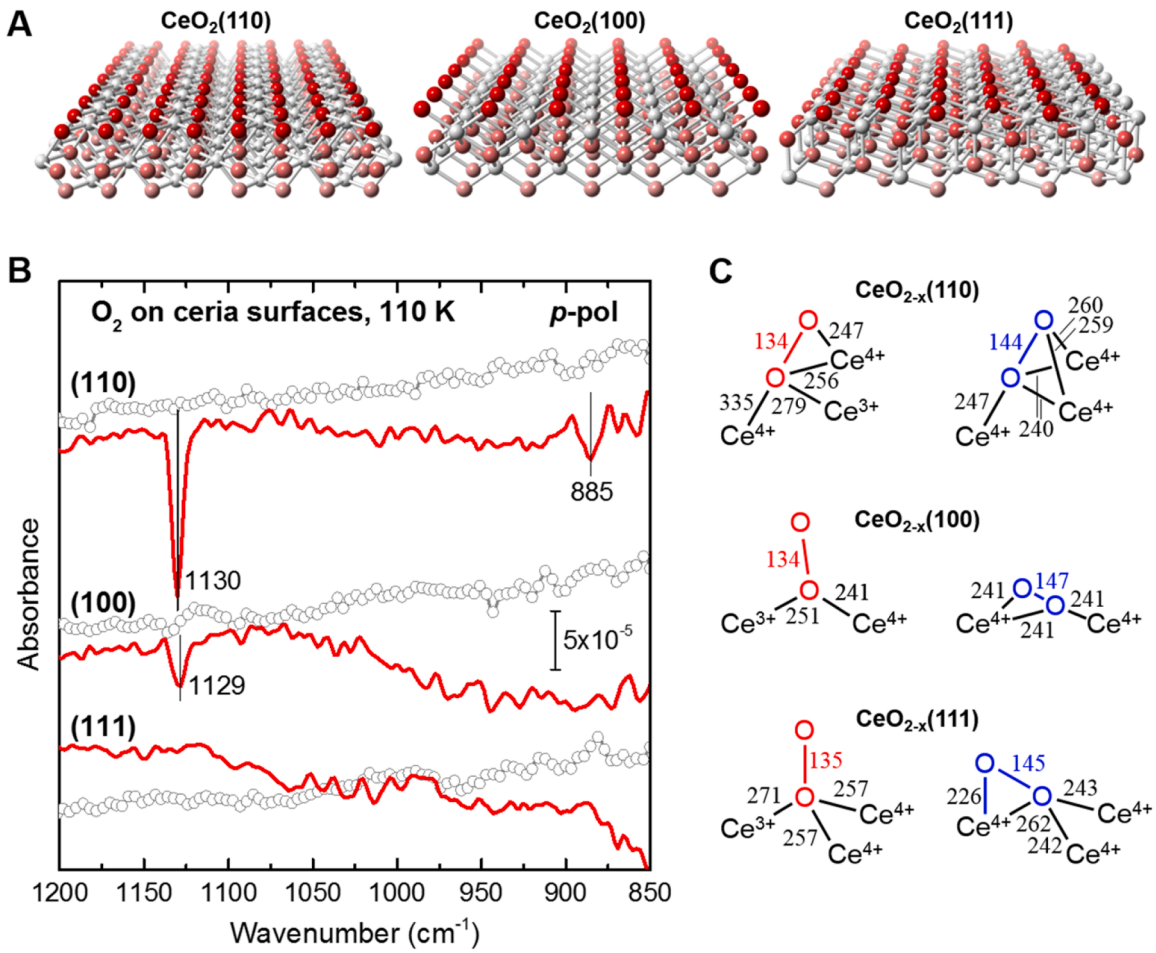

Fig. 3. Interactions of dioxygen with oxidized and reduced ceria surfaces. (A) Structural models of the low-index ceria surfaces. Deep red: surface O atoms, light red: subsurface O atoms, grey: Ce atoms. (B) IRRAS data recorded with p-polarized light after exposing the oxidized (black, open circle) and reduced (red, solid line) ceria (111), (110), and (100) surfaces to O_2 at 110 K. (C) Atomic structures of superoxide (red) and peroxide (blue) species formed on the reduced CeO_{2-x}(110), CeO_{2-x} (100), and CeO_{2-x} (111) surfaces. Bond lengths are given in pm. Reproduced from Ref. [34].

transport at elevated temperatures to yield (111)-dominated nano-pyramids [32]. It showcases a complex interplay between adsorbate vibrations and surface restructuring, which is crucial for understanding catalytic processes at the atomic level.

5. Comparison to the results of electronic structure calculations

The full set CO frequencies adsorbed on the different low-indexed crystallographic surfaces of ceria provides a unique chance to validate the results of electronic structure calculations. In the case of CO, while for the CeO_2 (111) surface a reasonable agreement was obtained already with fairly simple functionals (PBE) for CeO_2(110) surface, substantial deviation was observed between the results of experimental work which showed the typical blue-shifted signal and calculations using PBE which unexpectedly showed a red-shift relative to the gas phase signal (2143 cm^{-1}) [37]. A more thorough analysis [36] revealed that the strong deviation between experiment in theory in this case is an artefact from using simple functionals only when using hybrid functionals (HSE06). An excellent agreement between theoretical and experimental work can be achieved for all low-indexed surfaces of CeO_2, including the frequencies of CO adsorbed on reduced substrates. Note, that in these calculations the polarization-dependent shifts discussed above were not considered. A multi-method ab-initio approach used later to calculate these polarization-dependent changes in the position of vibrational bands of CO on CeO_2(111) showed excellent agreement with the experimental observed splitting [11].

6. Vibrational spectra of CO adsorbates at ambient pressure – towards operando studies

As noted in the introduction, the results of IRRAS studies on single crystals are needed for an analysis of powder data under ambient conditions. A successful realization of this approach has been demonstrated in recent work [26], where the vibrational bands of CO adsorbed on ceria powders could be detected at pressures of 1 atm using diffuse reflectance IR spectroscopy (DRIFTS). After carefully subtracting the contributions from the CO gas phase, the vibrations characteristic of the different crystallographic surfaces of ceria became visible (see Fig. 5). Interestingly, these measurements demonstrated that at such high pressures, reduction of the ceria powder particles occurs even at room temperature.

7. Conclusions and implications

The comprehensive application of IRRAS to study adsorbates on ceria single crystal surfaces has significantly advanced our understanding of surface-adsorbate interactions and the role of oxygen vacancies on this important metal oxide. These insights not only deepen our knowledge of ceria's catalytic mechanisms but also pave the way for the design and development of more efficient and targeted catalytic systems. The detailed vibrational analysis provides a microscopic view of the surface processes, crucial for optimizing ceria's performance in various industrial and environmental applications. Furthermore, with

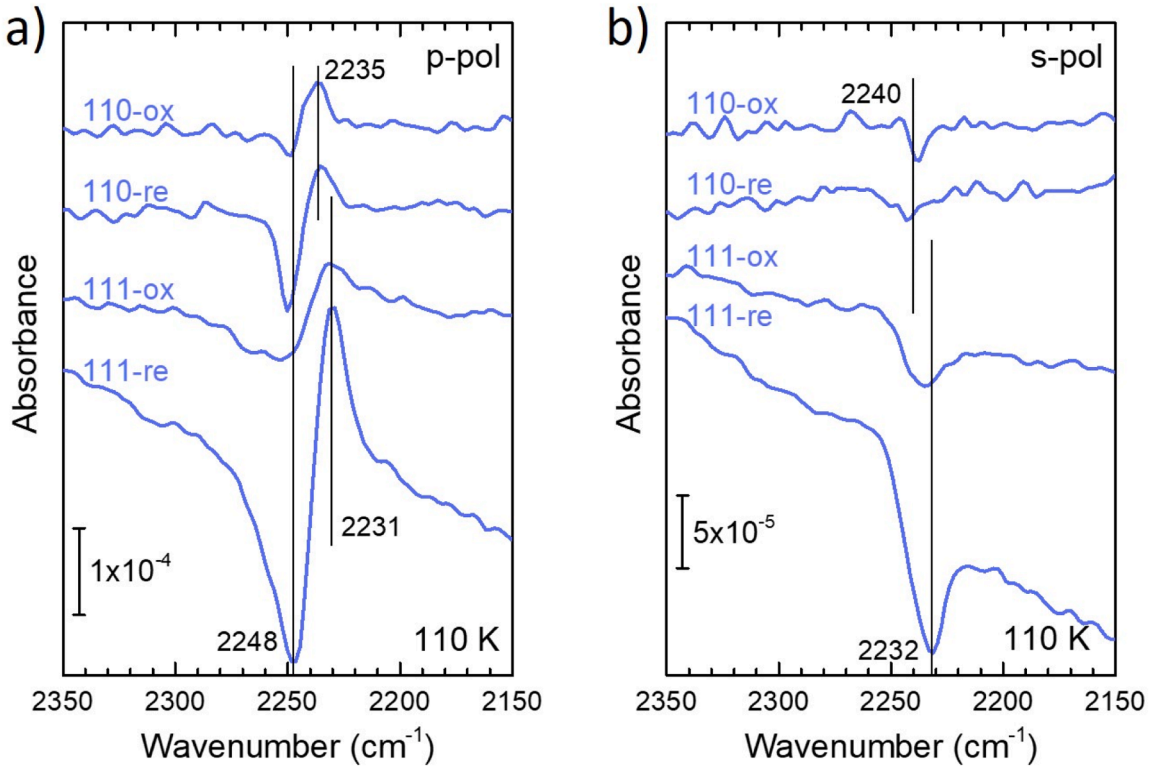

Fig. 4. Polarization-resolved IRRAS data of 1 ML N_2O adsorption on the oxidized and reduced (111) and (110) ceria surfaces at 110 K: (a) p-polarized spectra; (b) s-polarized spectra. Note the splitting of the vibrational bands in the left panel (polarization-dependent splitting, see text). Reproduced from Refs. [10] and [35].

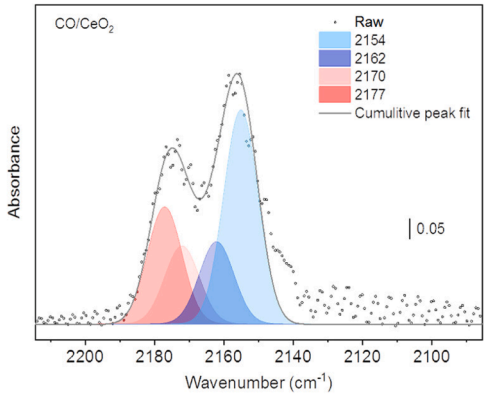

Fig. 5. Deconvoluted difference DRIFTS data (dotted line) of CO adsorbed on CeO_2 nanoparticles recorded at a CO pressure of 1 bar at 295 K. Note that the computation of the difference spectra requires a careful subtraction of the gas phase spectrum measured with high (2 cm^{-1}) resolution. Reproduced from Ref. [26].

the recently reported ability to detect CO adsorbate vibrations also at ambient pressures (CeO_2, [26] ZrO_2 [38]), operando studies will become possible, which will allow for an in-situ monitoring of chemical reactions in an operating reactor using the reference data obtained in UHV studies on single crystal surfaces.

CRediT authorship contribution statement

Chengwu Yang: Writing – original draft, Conceptualization. **Christof Wöll:** Writing – review & editing, Writing – original draft, Conceptualization.

Declaration of competing interest

There is no conflict of interest to declare on this paper.

Data availability

No data was used for the research described in the article.

Acknowledgement

This work was funded by the Deutsche Forschungsgemeinschaft (DFG, German Research Foundation) – Project-ID 426888090 – SFB 1441.

References

[1] M. Trenary, Reflection absorption infrared spectroscopy and the structure of molecular adsorbates on metal surfaces, Annu. Rev. Phys. Chem. 51 (2000) 381–403.
[2] C. Wöll, Structure and chemical properties of oxide nanoparticles determined by surface-ligand IR spectroscopy, ACS Catal. 10 (1) (2020) 168–176.
[3] J. Kattner, H. Hoffmann, External reflection spectroscopy of thin films on dielectric substrates, in Handbook of Vibrational Spectroscopy, in: J.M. Chalmers, P. R. Griffiths (Eds.), Handbook of Vibrational Spectroscopy, John Wiley & Sons, Chichester, 2002, pp. 1009–1027.
[4] B.E. Hayden, A. King, M.A. Newton, Fourier transform reflection–absorption IR spectroscopy study of formate adsorption on TiO_2(110), J. Phys. Chem. B 103 (1) (1999) 203–208.
[5] G. Ertl, H.J. Freund, Catalysis and surface science, Phys. Today 52 (1) (1999) 32–38.
[6] R.G. Greenler, D.R. Snider, D. Witt, R.S. Sorbello, The metal-surface selection rule for infrared-spectra of molecules adsorbed on small metal particles, Surf. Sci. 118 (3) (1982) 415–428.
[7] G.E. Becker, G.W. Gobeli, Surface studies by spectral analysis of internally reflected infrared radiation: hydrogen on silicon, J. Chem. Phys. 38 (12) (1963) 2942–2945.
[8] Y.J. Chabal, Surface infrared-spectroscopy, Surf. Sci. Rep. 8 (5–7) (1988) 211–357.

[9] M. Xu, Y. Gao, Y. Wang, C. Wöll, Monitoring electronic structure changes of TiO_2(110) via sign reversal of adsorbate vibrational bands, Phys. Chem. Chem. Phys. 12 (15) (2010) 3649–3652.
[10] C. Yang, Y. Cao, P.N. Plessow, J. Wang, A. Nefedov, S. Heissler, F. Studt, Y. Wang, H. Idriss, T.G. Mayerhöfer, C. Wöll, N_2O adsorption and photochemistry on ceria surfaces, J. Phys. Chem. C 126 (4) (2022) 2253–2263.
[11] B. Zerulla, M. Krstic, S. Chen, Z. Yu, D. Beutel, C. Holzer, M. Nyman, A. Nefedov, Y. Wang, T.G. Mayerhöfer, C. Wöll, C. Rockstuhl, Polarization-dependent effects in vibrational absorption spectra of 2D finite-size adsorbate islands on dielectric substrates, Phys. Chem. Chem. Phys. 26 (18) (2024) 13683–13693.
[12] Y.J. Chabal, K. Raghavachari, New ordered structure for the H-saturated Si(100) Surface - The (3×1) phase, Phys. Rev. Lett. 54 (10) (1985) 1055–1058.
[13] C. Yang, W. Wang, A. Nefedov, Y. Wang, T.G. Mayerhöfer, C. Wöll, Polarization-dependent vibrational shifts on dielectric substrates, Phys. Chem. Chem. Phys. 22 (30) (2020) 17129–17133.
[14] C. Yang, C. Wöll, IR spectroscopy applied to metal oxide surfaces: adsorbate vibrations and beyond, Adv. Phys.-X 2 (2) (2017) 373–408.
[15] N.V. Skorodumova, S.I. Simak, B.I. Lundqvist, I.A. Abrikosov, B. Johansson, Quantum origin of the oxygen storage capability of ceria, Phys. Rev. Lett. 89 (16) (2002) 166601.
[16] C.W.M. Castleton, J. Kullgren, K. Hermansson, Tuning LDA+U for electron localization and structure at oxygen vacancies in ceria, J. Chem. Phys. 127 (24) (2007) 244704.
[17] D.R. Mullins, The surface chemistry of cerium oxide, Surf. Sci. Rep. 70 (1) (2015) 42–85.
[18] T. Montini, M. Melchionna, M. Monai, P. Fornasiero, Fundamentals and catalytic applications of CeO_2-based materials, Chem. Rev. 116 (10) (2016) 5987–6041.
[19] A. Trovarelli, P. Fornasiero. Catalysis By Ceria and Related Materials, 2nd Edition, World Scientific Publishing Company, 2013.
[20] L. Vivier, D. Duprez, Ceria-based solid catalysts for organic chemistry, ChemSusChem. 3 (6) (2010) 654–678.
[21] J. Paier, C. Penschke, J. Sauer, Oxygen defects and surface chemistry of ceria: quantum chemical studies compared to experiment, Chem. Rev. 113 (6) (2013) 3949–3985.
[22] M. Nolan, S.C. Parker, G.W. Watson, The electronic structure of oxygen vacancy defects at the low index surfaces of ceria, Surf. Sci. 595 (1–3) (2005) 223–232.
[23] P. Pérez-Bailac, P.G. Lustemberg, M.V. Ganduglia-Pirovano, Facet-dependent stability of near-surface oxygen vacancies and excess charge localization at CeO_2 surfaces, J. Phys. Condens. Matter 33 (50) (2021) 504003.
[24] H.S. Gandhi, A.G. Piken, M. Shelef, Laboratory evaluation of three-way catalysts, SAE Tech. Pap. 55 (1976) 760201.
[25] S. Afrin, P. Bollini, On the utility of Ce^{3+} spin−orbit transitions in the interpretation of rate data in ceria catalysis: theory, validation, and application, J. Phys. Chem. C 127 (1) (2023) 234–247.
[26] L. Caulfield, E. Sauter, H. Idriss, Y.M. Wang, C. Wöll, Bridging the pressure and materials gap in heterogeneous catalysis: a combined UHV, in situ, and operando study using infrared spectroscopy, J. Phys. Chem. C 127 (29) (2023) 14023–14029.
[27] J.A. Rodriguez, D.C. Grinter, Z. Liu, R.M. Palomino, S.D. Senanayake, Ceria-based model catalysts: fundamental studies on the importance of the metal–ceria interface in CO oxidation, the water–gas shift, CO_2 hydrogenation, and methane and alcohol reforming, Chem. Soc. Rev. 46 (7) (2017) 1824–1841.
[28] G.H. Vurens, M. Salmeron, G.A. Somorjai, The preparation of thin ordered transition metal oxide films on metal single crystals for surface science studies, Prog. Surf. Sci. 32 (3) (1989) 333–360.
[29] G. Pacchioni, Two-dimensional oxides and their role in electron transfer mechanisms with adsorbed species, Chem. Record 14 (5) (2014) 910–922.
[30] C. Yang, L.-L. Yin, F. Bebensee, M. Buchholz, H. Sezen, S. Heissler, J. Chen, A. Nefedov, H. Idriss, X.-Q. Gong, C. Wöll, Chemical activity of oxygen vacancies on ceria: a combined experimental and theoretical study on CeO_2(111), Phys. Chem. Chem. Phys. 16 (44) (2014) 24165–24168.
[31] C. Yang, X. Yu, S. Heißler, A. Nefedov, S. Colussi, J. Llorca, A. Trovarelli, Y. Wang, C. Wöll, Surface faceting and reconstruction of ceria nanoparticles, Angew. Chem. Int. Edit. 56 (1) (2017) 375–379.
[32] C. Yang, M. Capdevila-Cortada, C. Dong, Y. Zhou, J. Wang, X. Yu, A. Nefedov, S. Heißler, N. López, W. Shen, C. Wöll, Y. Wang, Surface refaceting mechanism on cubic ceria, J. Phys. Chem. Lett. 11 (18) (2020) 7925–7931.
[33] C. Yang, F. Bebensee, A. Nefedov, C. Wöll, T. Kropp, L. Komissarov, C. Penschke, R. Moerer, J. Paier, J. Sauer, Methanol adsorption on monocrystalline ceria surfaces, J. Catal. 336 (2016) 116–125.
[34] C. Yang, X. Yu, S. Heißler, P.G. Weidler, A. Nefedov, Y. Wang, C. Wöll, T. Kropp, J. Paier, J. Sauer, O_2 Activation on ceria catalysts—the importance of substrate crystallographic orientation, Angew. Chem. Int. Edit. 56 (51) (2017) 16399–16404.
[35] C. Yang, X. Yu, P.N. Pleßow, S. Heißler, P.G. Weidler, A. Nefedov, F. Studt, Y. Wang, C. Wöll, Rendering photoreactivity to ceria: the role of defects, Angew. Chem. Int. Edit. 56 (45) (2017) 14301–14305.
[36] P.G. Lustemberg, C. Yang, Y. Wang, C. Wöll, M.V. Ganduglia-Pirovano, Vibrational frequencies of CO bound to all three low-index cerium oxide surfaces: a consistent theoretical description of vacancy-induced changes using density functional theory, J. Chem. Phys. 159 (3) (2023) 034704.
[37] P.G. Lustemberg, P.N. Plessow, Y.M. Wang, C.W. Yang, A. Nefedov, F. Studt, C. Wöll, M.V. Ganduglia-Pirovano, Vibrational frequencies of cerium-oxide-bound CO: a challenge for conventional DFT methods, Phys. Rev. Lett. 125 (25) (2020) 256101.
[38] S. Chen, P.N. Pleßow, Z. Yu, E. Sauter, L. Caulfield, A. Nefedov, F. Studt, Y. Wang, C. Wöll, Structure and chemical reactivity of Y-stabilized ZrO_2 surfaces: importance for the water-gas shift reaction, Angew. Chem. Int. Edit. 63 (27) (2024) e202404775.